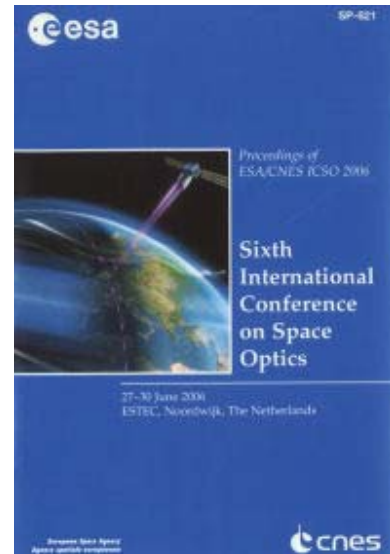


# International Conference on Space Optics—ICSO 2006

Noordwijk, Netherlands

27–30 June 2006

*Edited by Errico Armandillo, Josiane Costeraste, and Nikos Karafolas*



## *High resolution measurements of solar induced chlorophyll fluorescence in the Fraunhofer oxygen bands*

*M. Mazzoni, G. Agati, G. Cecchi, G. Toci, et al.*



## HIGH RESOLUTION MEASUREMENTS OF SOLAR INDUCED CHLOROPHYLL FLUORESCENCE IN THE FRAUNHOFER OXIGEN BANDS

M. Mazzoni<sup>(1)</sup>, G.Agati<sup>(1)</sup>, G.Cecchi<sup>(1)</sup>, G.Toci<sup>(1)</sup>, P.Mazzinghi<sup>(2)</sup>

<sup>(1)</sup>IFAC, via Madonna del Piano, 50019 Sesto Fiorentino (Fi), Italy, e-mail M.Mazzoni@ifac.cnr.it

<sup>(2)</sup>INOA, Largo E. Fermi 6, 50125 (Fi), Italy

### ABSTRACT

Spectra of solar radiance reflected by leaves close to the Fraunhofer bands show the net contribution of chlorophyll fluorescence emission which adds to the reflected solar spectra. In a laboratory experiment, a low stray light, high resolution, 0.85 m double monochromator was used to filter radiation living leaves still attached to the plant in correspondence of the 687 nm and 760 nm O<sub>2</sub> absorption bands. Reference spectra from a non fluorescent white reference were also acquired. Acquisition was performed by a Microchannel plate (MCP) intensified diode array with 512 elements. A fit of the spectral data outside the absorption lines allowed to retrieve the spectral base-line as a function of wavelength for the reference panel and the leaf. Reflectance functions were determined extending the Plascyck equation system [1] to all the resolved lines of the oxygen absorption bands and using the base-lines for the continuum values. Fluorescence was deduced from the same equation system, using both the measured leaf and reference radiance spectra and the leaf reflectance fitting function.

### 1. CHLOROPHYLL FLUORESCENCE AND LEAF REFLECTANCE SIGNALS

Experiments for the observation of solar induced chlorophyll fluorescence signals are one of the main issues of recent campaigns (SEN2FLEX). In the region of high solar radiation absorption, fluorescence is likely to be detected with better signal-to-noise ratio for the attenuation of the reflected solar spectrum. Fluorescence experiments (AIRFLEX) in the O<sub>2</sub>-A band and O<sub>2</sub>-B band are currently performed with a spectral resolution of 1nm and 0.5 nm, respectively [2]. Reflectance measurements at 687 nm and 760 nm are used to deliver the Normalised Difference Vegetation index (NDVI) for the evaluation of the density of the green mass. Reflectance measurements at 531 nm and 570 nm are also used to give the Physiological Reflectance Index (PRI) correlated with a non-

photochemical quenching [3]. In these experiments, the spectral resolution is generally low and the instruments deliver an integrated value of reflectance in correspondence of the absorption bands. Also the reflectance of the reference target, which is measured outside the absorption bands and is used in the Plascyck formula [1] to deliver fluorescence, is measured with the same spectral resolution. In this paper we show that with high resolution measurements, in the proximity of the Fraunhofer oxygen bands, it is possible to process complete spectra, of solar radiance from the reference panel and of leaf radiance, to give accurate lineshapes of both reflectance and fluorescence. Chlorophyll fluorescence is well known as indicator of photosynthetic activity and vegetation health state [4, 5, 6]. Furthermore, as the shape variation of the red-edge region (from 650 nm to 800 nm) of vegetation spectra were proved to be correlated to the stresses induced on the leaf [7], high resolution reflectance spectra are useful by themselves and also for the correct interpretation of the fluorescence signal [8].

### 2. EXPERIMENTALS

The measurements were performed on single leaves attached to plants using a Spectralon standard (Labsphere, North Sutton, NH) for the reference panel. The fluorescence emission and the reflected radiance from leaves of *Lycopersicon esculentum*, *Cucurbita pepo*, *Cucumis sativus*, and *Epipremnum aurea* plants were collected by a silica fibre and dispersed with a double monochromator.

Filtered light was imaged on the 512 channels of an MCP intensified 1420 sensor head, with pixels 25 µm wide, of an Optical Multichannel Analyzer (OMA 3 EG&G), in single scan acquisitions of 12 s-15 s. This single scan time duration was chosen to get sufficient dynamic of the integrated signal with respect to the noise level during the daily solar irradiance. Solar irradiances with sun sited from zenith to about 45 degree were considered. Measurements were performed in Florence, in the June – August months of the year 2005. The photosynthetic photon flux density (PPFD) was measured by means of a multimeter equipped with a Quantum LI-COR head. From 12 a.m. to 5 p.m., this

value varied about from 1100 to 300  $\mu\text{mol s}^{-1} \text{m}^{-2}$ . The signal background obtained with the monochromator slits closed was subtracted both to reference and leaf acquisitions for each scan. The fibre tip was placed at the entrance slit of the double monochromator. Typically, an entrance slit height of 1 cm was used, which corresponded to a compromise between signal enhancement and stray-light reduction on the sensor. The symmetry of the diffracted pattern of the sunlight collected by the fibre was controlled by means of the double monochromator aiming view optics, which images the entrance slit and at the exit slit. Furthermore, the width of the entrance slit was opened to 40-50  $\mu\text{m}$ . This width corresponded to an almost 1:1 configuration with the “two-pixel” equivalent response width of the sensor array to a delta function, which was deduced from the line-shape of a He-Ne laser spectrum measured with the monochromator entrance slit set to 10  $\mu\text{m}$ . According to the number of lines (1200 lines/mm) of the two monochromator holographic gratings, the resolution resulted of about 0.03 nm (convolution of monochromator resolution and sensor array cross-talk) and the spectral range imaged onto the pixel array about 5 nm in the red region of interest. The sensor was cooled at  $-15^\circ\text{C}$  to optimise signal-to-noise ratio while preventing the sealing optics fogging at the maximum admitted flow of the  $\text{N}_2$  purging gas. The OMA signals were stored on a PC equipped with a graphic interface (LabView) for the acquisition and display of the single acquisitions. After signal maximisation with monochromator set for maximum transmission at the centre of the MCP imaged spectral range, a calibration was performed with a reference lamp.

### 3. SIGNAL PROCESSING

We processed the signals outside and inside the absorption lines separating the pixels into two groups of different origin. Using the signals in the spectral ranges outside the absorption lines for a linear fit, this procedure allowed us to derive a continuous base-line for both the reference panel and the leaf.

The radiance spectra of the white standard and of the leaf under solar illumination in correspondence of the 685 nm  $\text{O}_2$  absorption band are shown in Figs. 1 and 2, respectively, divided by the calibration curve of the reference lamp. In the reference panel spectrum, all the roto-vibrational lines appear almost completely resolved and the fitted base-line (linear function) is shown in Fig. 1 along with the calibrated solar spectrum. To fit the base-line of the leaf spectrum with a linear fit, only two spectral ranges (in correspondences of the two extremes of the spectrum) can be used. The resulting fit is shown in Fig. 2 along with the calibrated leaf radiance spectrum.

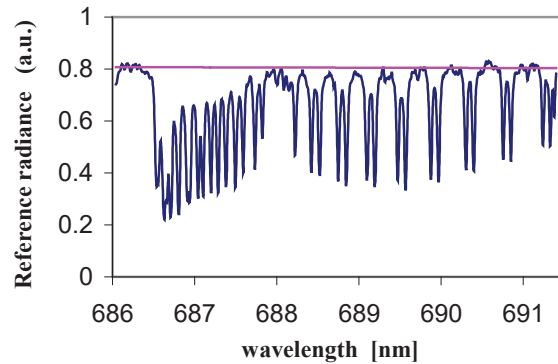


Fig. 1. Solar spectrum in the  $\text{O}_2$  absorption band. Radiance from the reference panel and fitted base-line (straight line).

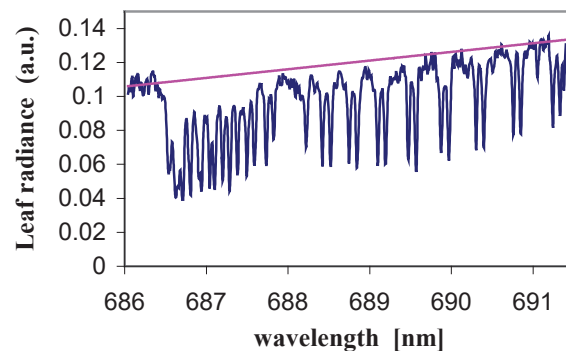


Fig. 2. *Cucurbita pepo* leaf radiance spectrum with the linear fit of the base-line.

The linear fit for the leaf radiance penalises the accuracy deriving from the use of more spectral ranges to determine the base-line, because the reflectance spectra of a leaf cannot be considered linear even in the limited spectral range under investigation. The fit shown in Fig. 3 is a second order curve obtained considering eight significant spectral ranges, the same considered for the reference spectrum.

The leaf base-line shape depends on the variability of both reflectance and fluorescence as a function of the wavelength and can be used to derive the slope of the dominant effect with a propagated error which is two times higher than the uncertainty of the single radiance measurement.

The leaf spectrum, normalised to the baseline, is shown in Fig. 4. It can be used to compare the absorption line depths with those of the reference panel spectrum shown in Fig. 5.

To infer the reflectance of the leaf as a function of wavelength, the spectra were compared to the fitted base-line values for each wavelength.

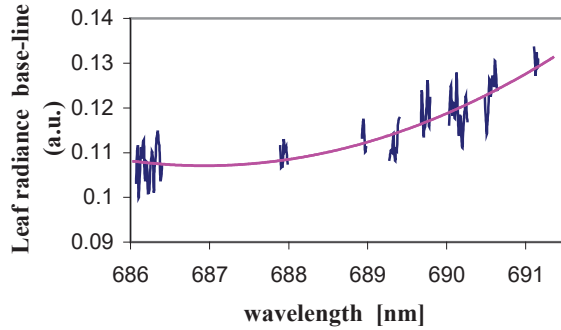


Fig. 3. Leaf data used to fit the leaf spectrum base-line with a second order function (continuous line).

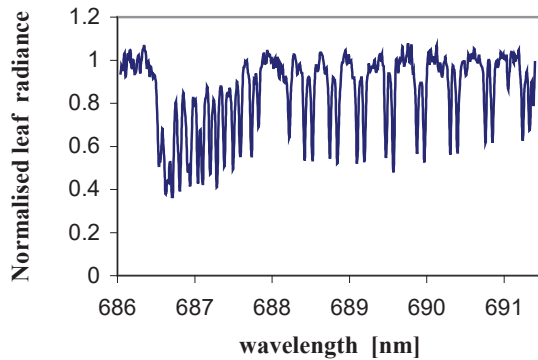


Fig. 4. Leaf spectrum, normalised to the base-line.

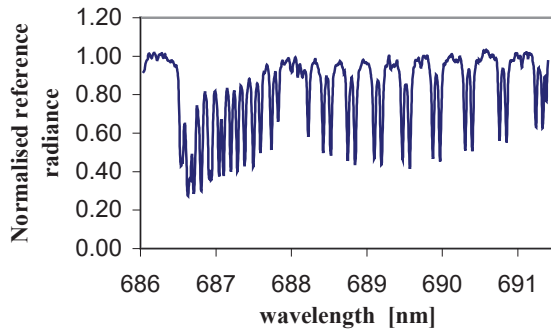


Fig. 5 Reference panel spectrum normalised to the base-line.

In particular, according to [1], we used the following relationship to compute the ratio  $R(\lambda)$  between the energy flux reflected by the sample in a given solid angle and the energy flux reflected by the reference target in the same solid angle:

$$R(\lambda) = \frac{LB(\lambda) - LS(\lambda)}{RB(\lambda) - RS(\lambda)} \quad (1)$$

In (1), LB and RB are the leaf and reference spectrum base-lines, LS and RS are the leaf and reference spectra, respectively.

In the calculation, only the data inside the absorption lines were taken into account to avoid the artefacts deriving from a null denominator in correspondence of the spectral ranges used to fit the base-line. In Fig. 6 we report the fit of  $R(\lambda)$  which we used for the calculation of fluorescence and the data used to fit the spectrum base-line. The propagated error for  $R(\lambda)$  was four times the uncertainty of a radiance measurement. Even if  $R(\lambda)$  can be obtained without any spectrum calibration, as it results from the ratio of signals detected with the same instrument, the derivation of fluorescence absolute values needs this operation.

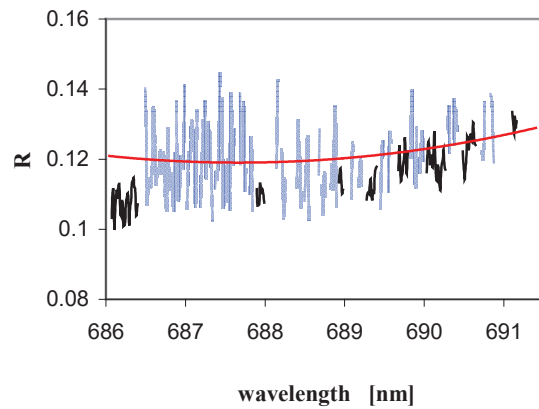


Fig. 6. Data groups of  $R(\lambda)$  values within the oxygen absorption lines (light lines) and their global fit (second-order-function continuous line), along with the leaf spectral data used to find the base-line (dark lines).

In fact, fluorescence [1] was deduced as:

$$F(\lambda) = LS(\lambda) - FITR(\lambda)RS(\lambda) \quad (2)$$

where  $FITR(\lambda)$  is the fit of  $R(\lambda)$ . The propagated error for fluorescence is six times the uncertainty of a radiance measurement. To test the effectiveness of the procedure we measured the signal from the front and the back sides of the leaf. The two spectra were probably differing for the different reabsorption of fluorescence [9].

They are reported in Fig. 8 along with the second order functions that fit each data set. A more restrictive selection of these does not substantially reduce the differences, as the spectra remained perfectly distinguishable within errors. The front fluorescence in the 687 nm absorption band resulted about 20% of leaf spectrum continuum, and about 2.5% of the solar

spectrum continuum diffused by the reference panel and collected by the fibre. The fluorescence intensity corresponded to about 20 mW/m<sup>2</sup>/nm.

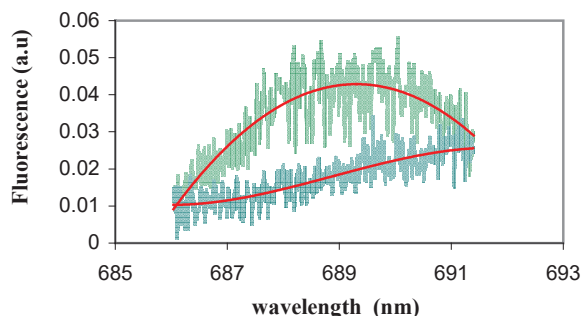


Fig. 8. Front (lower spectrum) and back (upper spectrum) leaf fluorescence spectra and fits (second order function, continuous lines).

The front and back leaf spectra have almost the same line shape at 760 nm, as expected from the extremely reduced influence of fluorescence reabsorption at this wavelength. In Fig. 9 we report the leaf front radiance at this wavelength, along with  $F(\lambda)$  and its linear fit. In this case  $R(\lambda)$  is an almost constant value equal to 0.37. Fluorescence resulted about 2.5% of the leaf radiance spectrum continuum and about 1% of the reference solar spectrum continuum, for a corresponding fluorescence intensity of about 4mW/m<sup>2</sup>/nm.

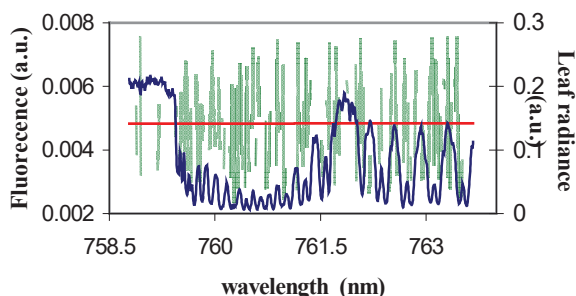


Fig. 9. Front leaf radiance spectrum (dark line), fluorescence (light line) and fluorescence linear fit (continuous line).

The values of the sun-excited fluorescence in the O<sub>2</sub> bands, that we found for leaves attached to plants, are consistent with those predicted by the FLEX community.

#### 4. CONCLUSIONS

This preliminary experiment demonstrates the advantages of using a high resolution, low stray-light,

spectrometer for the evaluation of the sun-excited fluorescence in the Fraunhofer bands. The increase in the precision of the evaluation of the relative contribution of the fluorescence and the reflected radiance is particularly useful in the atmospheric oxygen bands. In fact, when this measurement is done from a spacecraft outside the Earth atmosphere, the contributes of atmospheric absorption on the incoming solar radiance and on reabsorption of the fluorescence emission must be precisely evaluated to retrieve the fluorescence signal at ground.

#### 5. REFERENCES

1. Plascyck J.A. The MK II Fraunhofer line discriminator (FLD-II) for airborne and orbital remote sensing of solar-stimulated luminescence, *Opt. Eng.*, Vol. 14, 339-346, 1975.
2. <http://www.uv.es/leo/sen2flex/welcome.htm>
3. Alonso L., Moreno J., Moya I., Miller J. R. A comparison of different techniques for passive measurement of vegetation photosynthetic activity: solar-induced fluorescence, red-edge reflectance structure and photochemical reflectance indices, GeoScience and Remote Sensing Symposium 2003, IGARS '2003, *Proceedings. 2003 IEEE International*, Vol. 1, 21-25 July 2003, 604-606 (and reference therein).
4. Cecchi G., Mazzinghi P., Pantani L., Valentini R., Tirelli D., De Angelis P. Remote sensing of chlorophyll fluorescence on vegetation canopies: 1. near and far field measurement techniques, *Remote Sens. Environ.*, Vol 47., 18-28, 1994.
5. Valentini R., Cecchi G., Mazzinghi P., Scarascia Mugnozza G., Agati G., Bazzani M., De Angelis P., Fusi F., Matteucci G., Raimondi V. Remote sensing of chlorophyll fluorescence on vegetation canopies: 2. Physiological significance of fluorescence signal in response to environmental stresses, *Remote Sens. Environ.*, Vol. 47, 29-35, 1994.
6. Agati G., Mazzinghi P., Fusi F., Lipucci di Paola M., and Cecchi G. The F685/F730 chlorophyll fluorescence ratio as a indicator of chilling stress in plants, invited paper, *J. Plant Physiol.*, Vol. 148, 384-390, 1996
7. Zarco-Tejada P.J., Pushnik J.C., Dobrowski S., Ustin S.L. Steady-state chlorophyll a fluorescence detection from canopy derivative reflectance and double-peak red-edge effects, *Remote Sensing of Environment*, Vol. 84, 283-294, 2003.
8. Agati G., Fusi F., Mazzinghi P., Lipucci Di Paola M. A simple approach to evaluate the reabsorption of chlorophyll fluorescence spectra in intact leaves, *J. Photochem. Photobiol.*, Vol. 17, 163-171, 1993.
9. Louis J. , Cerovic Z.G., Moya I., J. Photochem. *Photobiol. B: Biol.*, 2006, in press (and references therein).